Analysis of White Noise on Power Frequency Estimation by DFT-based Frequency Shifting and Filtering Algorithm

Terms of use:

Analysis of White Noise on Power Frequency Estimation by DFT-based Frequency Shifting and Filtering Algorithm

Junhao Zhang, *Student Member*, *IEEE*, Lu Tang, Alessandro Mingotti, *Student Member*, *IEEE*,
Lorenzo Peretto, *Senior Member, IEEE*, and He Wen, *Member, IEEE*

Abstract—**The frequency shifting and filtering (FSF) algorithm, a variant of DFT, has the merit of high efficiency for frequency analysis thanks to its simple implementation in the time domain. However, the inevitable white noise injected by various factors leads to inaccurate frequency estimation in practical measurement. This paper investigates the influence of a stationary white noise on FSF-based frequency estimation of the power system. The variance expression of the frequency estimator is derived theoretically and compared to its unbiased Cramer-Rao Lower Bound (CRLB). The obtained results are validated by several computer simulations.**

Index Terms—**Variance analysis, Frequency shifting, Filtering, Signal to noise ratio, Cramer-Rao Lower Bound.**

I. INTRODUCTION

The frequency is a significant indicator for the monitoring, control, and protection of the power system. Accurate frequency estimation can better reflect the status of the power system and provide a reliable basis for the operation of the grid [1, 2]. As the ever-increasing demand for renewable power, the power quality of the power system continues to deteriorate because of the large number of power electronics used in connections of the new power. Thus, a fast and accurate frequency estimation method is required strongly for the safety, stability, and efficiency of the power system [3].

In recent decades, various digital signal processing techniques, such as Discrete-Fourier-transform (DFT), DFT-based methods, Phase-locked loop, Notch filter, Prony's method, zero-crossing method, wavelet transform, least-squared technique, Kalman filter, Taylor method, Newton's method and Artificial neural network, have been published in scientific literature to provide methods for estimating frequency [4-8]. However, the difficulty of

J. Zhang, H. Wen, and L. Tang are with the College of Electrical and Information Engineering, Hunan University, and also with the Hunan Province Key Laboratory of Intelligent Electrical Measurement and Application Technology, Changsha City 410082, China. (e-mail: luoyzjh@163.com, he_wen82@126.com, tangl@126.com)

A. Mingotti, and L. Peretto are with the Department of Electrical, Electronic and Information "Guglielmo Marconi," Alma Mater Studiorum, University of Bologna, 40126 Bologna, Italy (e-mail: alessandro.mingotti2@unibo.it; lorenzo.peretto@unibo.it).

guaranteeing the synchronous sampling prevents the classical algorithms from being a good selection for accurate frequency estimation. In addition, a lot of effort has been paid to raise the performance of these classical methods under asynchronous sampling. Among them, the windowed interpolation Fast Fourier Transform (WIFFT), one variant of DFT, is widely used because it well addresses the spectrum leakage and picket fence effect caused by asynchronous sampling through time domain windowing and frequency domain interpolation [9] [10]. Furthermore, diverse window functions and interpolation method are proposed to enhance the performance of WIFFT. However, the tradeoff between the length of window and accuracy makes it hardly fulfill the accuracy requirement of frequency estimation when few samples can be collected.

To improve the performance of DFT, an effective method named Frequency Shifting and Filtering (FSF) algorithm is proposed to estimate the frequency [11]. The FSF only employs two main steps, by starting from the raw data: frequency shifting by the reference signal (similar to the heterodyne action of WIFFT) and iterative filtering (similar to the windowing action of WIFFT) based on the averaging filter, to process the raw data. Thus, the FSF can be seen as a conventional DFT with a filter/window consisting of a cascade of L rectangular windows, each with an equal and fixed number of samples, equivalent to one period at nominal system frequency. With frequency shifting and filtering implemented only in the time-domain, a satisfactory frequency estimation can be obtained, while the conventional WIFFT method needs an interpolation process in frequency domain to lower the inherent defect picket fence effect. Thus, the benefits of an FSF implementation consist of higher efficiency and accuracy on estimating the frequency (in asynchronous sampling) compared with the widely-used WIFFT [12].

It is worth noting that the accuracy of frequency estimation is not only affected by the used algorithm but also by the white noise contained in the sampled signal. When the contribution of white noise becomes significant, the performance of the algorithm under noisy condition must be re-evaluated and tested. On the contrary, if the signal-to-noise ratio (SNR) is higher enough, which means that the influence of the noise on frequency estimation is negligible, the attention is moved to the evaluation of the measurement error produced by the algorithm itself [13, 14].

As for the noise, among the grid, a Low Voltage (LV) distribution system typically contains more noise than the High

Voltage (HV) one. According to [15, 16], the background noise of LV distribution system can be considered as white noise. [17] points that the SNR of distribution level grid signals is about 60-70dB. Although the acquired samples will be filtered first, the noise level can still be high enough to pollute the frequency estimation. In addition, the transducers and acquisition circuit used in the measurement equipment, e.g., Phasor Measurement Unit (PMU), power quality analyzer, will also introduce the noise which affects the accuracy of frequency estimation. [18] gives the principle of how the analog instrumentation and quantization effects introduce the white noise. Therefore, the inherent and introduced noise existed in the sampled signal of the power system can be treated as the Additive White Gaussian Noise (AWGN). Thereby performance of the frequency estimators adopted in the power system needs to be evaluated under AWGN pollution [19].

Moving to other well-known methods and approaches, a zero-crossing-based method for the estimation of the frequency of a single sinusoid in white noise is presented in [20]. The performance of an extended Kalman filter approach for the frequency measurement of noisy power system signals has been evaluated and presented in [21]. With regard to the famous DFT, there are a lot of noise-related researches in the existing literature. The effect of window functions on the uncertainty of the DFT-based frequency estimator under noisy condition is investigated in [22] and [23]. The noise effect on the power system frequency measurement is analyzed in [24] and [17]. The difference is that, [24] uses the triangular self-convolution window based double line interpolation DFT, while [17] adopts the triple-line interpolation DFT with combined cosine windows. In [25], the effects of noise on the detection and estimation of weak sine waves caused by analog-to-digital conversion and windowing is tackled. [26] applies three digital filters with second-degree integrators to reduce the noise effect for frequency estimation based on DFT method. [18] analyzes the effect of white noise onto frequency estimation based on the filtered heterodyned measurement which is basically the same as the so-called FSF in this paper. Based on its conclusion, a cascade of two roughly equal length boxcar filters is suggested for frequency measurement. However, to the authors' knowledge, the expression about the effect of white noise on frequency estimation based on FSF with a varying measurement interval has not been given in [18] nor the published literature.

In this paper, the influence of white noise on measurement errors of FSF-based frequency is firstly examined theoretically; then, the frequency variance expression is derived in two cases according to the interval between two adopted measuring samples. The correctness of variance expression is finally verified by several designed simulations on Matlab software.

The paper is structured as follows: Section II recalls the procedure of FSF on the power system frequency estimation. Section III analyzes the frequency variance based on FSF, and the variance expression is given with respect to SNR. Moreover, it contains the comparison between frequency variance and the unbiased Cramer-Rao Lower Bound (CRLB). Section IV provides the simulation tests and results which can verify the proposed expressions. Finally Section V discusses the conclusion.

II. FREQUENCY ESTIMATION BASED ON FSF

Applying FSF to estimate the power system frequency as shown in [11] requires the following 6 steps.

STEP 1, acquiring the power system signal distorted by harmonic content with sampling frequency f_s as:

$$x(n) = \sum_{h=1}^{H} A_h \sin\left(2\pi n f_h / f_s + \theta_h\right) \tag{1}$$

where H is the highest order of harmonic; A_h, θ_h, and f_h represent the amplitude, phase, and frequency of the hth harmonic, respectively. In particular, A_1, θ_1, and f_1 are the corresponding parameters of the signal fundamental component; $f_s = D f_r$, where D is an integer number, f_r is the nominal frequency of the power system, i.e., 50 Hz or 60 Hz. $n=0,1,2,3,\ldots,N\text{-}1$, where N is the number of acquired samples. By considering an In-field signal, there will be a deviation Δf between f_r and f_1 actually, i.e., $\Delta f = f_r - f_1$, and $\Delta f \ll f_1$ usually.

STEP 2, generating a reference signal $r(n)$ with frequency f_r expressed as (2) for the power frequency f_1 estimation.

$$r(n) = e^{j\frac{2\pi n f_r}{f_s}} = e^{j\frac{2\pi n}{D}} \tag{2}$$

where j is the imaginary unit.

STEP 3, frequency shifting $x(n)$ using $r(n)$ as:

$$s(n) = x(n) \cdot r(n)$$
$$= \sum_{h=1}^{H} \frac{A_h}{2j}\left(e^{j\theta_h} e^{j2\pi n(f_h + f_r)/f_s} - e^{-j\theta_h} e^{j2\pi n(f_r - f_h)/f_s}\right) \tag{3}$$

where $s(n)$ is called the frequency shifted signal.

According to (3), it is clear that after frequency shifting, $f_r - f_1 = \Delta f$ is the only component which can be approximately 0Hz. Thus, if Δf is known with a low uncertainty, f_1 can be obtained with high accuracy.

STEP 4, filtering out the undesired components in $s(n)$ using the averaging-filter-based Equivalent Weighting Filter (EWF) as:

$$s^L(n) = \sum_{i=n}^{K-1+n} s(i) \cdot w_{eq}(i-n+1)$$
$$= \sum_{h=1}^{H} \frac{A_h}{2}\left|G(\omega_{h\text{-Neg}})\right|^L e^{j[(\omega_{h\text{-Neg}}n - \theta_h + \frac{\pi}{2}) + \frac{L(D-1)}{2}\omega_{h\text{-Neg}}]}$$
$$+ \sum_{h=1}^{H} \frac{A_h}{2}\left|G(\omega_{h\text{-Pos}})\right|^L e^{j[(\omega_{h\text{-Pos}}n + \theta_h - \frac{\pi}{2}) + \frac{L(D-1)}{2}\omega_{h\text{-Pos}}]} \tag{4}$$

where $\omega_{h\text{-Pos}} = 2\pi(f_r + f_h)/f_s$ and $\omega_{h\text{-Neg}} = 2\pi(f_r - f_h)/f_s$ are the sampling angle differences of the positive and negative frequency components of the hth harmonic, respectively. L is the times of iterative filtering, $G(\omega)$ is the magnitude response of the averaging filter. $w_{eq}(n)$ is the EWF shown as (5) and $K = L(D-1)+1$ is the order of EWF.

$$w_{eq}(n) = \underbrace{w(n) * w(n) * \cdots * w(n)}_{L} \tag{5}$$

Notation	Meaning	Notation	Meaning
f_r	Nominal frequency of the power system	N	Number of samples
D	An integer related to sampling frequency	M	Measurement interval
L	Iteration times of FSF	n_1	The first measuring point
K	Order of the EWK	n_2	The second measuring point

where '*' means convolution operation, $w(n)$ is the Dth order averaging filter.

After the filter application, only the component $\omega_{1\text{-Neg}}$ remains, while all the other components of $s(n)$ are suppressed to 0 roughly. Thus, $s^L(n)$ shown in (4) is simplified as:

$$s^L(n) \approx \frac{A_1}{2}\left|G(\omega_{1\text{-Neg}})\right|^L e^{j[(\omega_{1\text{-Neg}}n-\theta_1+\frac{\pi}{2})+\frac{L(D-1)}{2}\omega_{1\text{-Neg}}]} \quad . \quad (6)$$

STEP 5, calculating the sampling angle difference $\omega_{1\text{-Neg}}$ of two samples in $s^L(n)$ with interval M using the following equation.

$$\omega_{1\text{-Neg}} = \frac{\arg\left(s^L(n_2)\right) - \arg\left(s^L(n_1)\right)}{M} \quad (7)$$

where arg( ) represents the angle of a complex number, $M=n_2-n_1$, is the measurement interval.

STEP 6, estimating the power system frequency f_1 by:

$$f_1 = \frac{2\pi - D\omega_{1\text{-Neg}}(n_1)}{2\pi}f_r \quad (8)$$

III. ANALYSIS OF WHITE NOISE ON THE POWER FREQUENCY ESTIMATION

In this section, the influence of the AWGN on power frequency estimation provided by FSF [11] is investigated. The variance expression of the power frequency estimation based on FSF is analyzed and derived theoretically. In addition, the ratio between the theoretical variance and its CRLB is analyzed.

Let us define $y(n)$ as a pure sinusoidal signal corrupted by AWGN $z(n)$ with zero mean and variance σ^2:

$$y(n) = x(n) + z(n) \quad (9)$$

where $x(n)$ is the pure sine wave with frequency f_1, amplitude A_1 and phase angle θ_1.

After being frequency shifted by $r(n)$ of frequency f_r, the frequency shifted signal $s(n)$ is expressed as:

$$s(n) = (x(n) + z(n)) \cdot r(n) \quad (10)$$

Then $s(n)$ is filtered by EWF $w_{eq}(n)$ using (4). For the sake of simplicity, $s^L(n)$ is expressed by a complex vector as:

$$V_S(n) = V_{1\text{-Neg}}(n) + V_{1\text{-Pos}}(n) + V_z(n) \quad (11)$$

where $V_S(n)$ is the complex vector of $s^L(n)$; $V_{1\text{-Neg}}(n)$ and $V_{1\text{-Pos}}(n)$ are the negative and the positive components while $V_Z(n)$ is the filtered AWGN. All can be presented as follows:

$$V_Z(n) = \sum_{i=n}^{K-1+n}\left[w_{eq}(i-n+1)\cdot z(i)\cdot e^{j\frac{2\pi i}{D}}\right] = B\angle\varphi_Z(n) \quad (12)$$

$$\begin{cases} V_{1\text{-Neg}}(n) = A_N\angle\varphi_N(n) \\ A_N = \frac{A_1}{2}\left[H(\omega_{1\text{-Neg}})\right]^L \\ \varphi_N(n) = \omega_{1\text{-Neg}}n - \theta_1 + \frac{\pi}{2} + \frac{L(D-1)}{2}\omega_{1\text{-Neg}} \end{cases} \quad (13)$$

$$\begin{cases} V_{1\text{-Pos}}(n) = A_P\angle\varphi_P(n) \\ A_P = \frac{A_1}{2}\left[H(\omega_{1\text{-Pos}})\right]^L \\ \varphi_P(n) = \omega_{1\text{-Pos}}n + \theta_1 - \frac{\pi}{2} + \frac{L(D-1)}{2}\omega_{1\text{-Pos}} \end{cases} \quad (14)$$

where $\varphi_N(n)$, $\varphi_P(n)$ and $\varphi_Z(n)$ represent the angle of $V_{1\text{-Neg}}(n)$, $V_{1\text{-Pos}}(n)$ and $V_Z(n)$, respectively, and B is the module of $V_Z(n)$.

According to the characteristics of the AWGN adopted, it results that the expectation and variance of $V_Z(n)$ are:

$$E\{V_Z(n)\} = \sum_{i=n}^{K-1+n} E\{w_{eq}(i-n+1)z(i)\}\cdot e^{j\frac{2\pi i}{D}} = 0 \quad (15)$$

$$\text{Var}\{V_Z(n)\} = E\{V_Z(n)^2\} = K\sigma^2\cdot NNPG \quad (16)$$

where $NNPG$ is the Normalized Noise Power Gain defined as:

$$NNPG = \frac{1}{K}\sum_{n=1}^{K}\left[w_{eq}(n)\right]^2 \quad (17)$$

Due to the frequency response of the adopted iterative filtering process, $V_{1\text{-Pos}}(n)$ is negligible compared with $V_{1\text{-Neg}}(n)$, thereby $V_S(n)$ can be written as:

$$V_S(n) \approx V_{1\text{-Neg}}(n) + V_z(n) = A_N\angle\varphi_N(n) + B\angle\varphi_Z(n)$$

$$= A_N\angle\varphi_N(n)\left[1 + \frac{B}{A_N}\angle(\varphi_Z(n) - \varphi_N(n))\right] \quad (18)$$

Moreover, $V_S(n)$ can be represented as:

$$V_S(n) = A_S(n)\angle\eta(n) \quad (19)$$

where $A_S(n)$ and $\eta(n)$ are the module and the angle of $V_S(n)$, respectively, which can be expressed as:

$$A_S(n) = A_N\left[1 + \left(\frac{B}{A_N}\right)^2 + \frac{2B}{A_N}\cos(\varphi_Z(n) - \varphi_N(n))\right]^{\frac{1}{2}} \quad (20)$$

$$\eta(n) = \varphi_N(n) + \arctan\left[\frac{\frac{B}{A_N}\sin(\varphi_Z(n) - \varphi_N(n))}{1 + \frac{B}{A_N}\cos(\varphi_Z(n) - \varphi_N(n))}\right] \quad (21)$$

Under the assumption of SNR>>1, it results that $B/A_N<<1$, hence, $\eta(n)$ can be simplified as:

$$\eta(n) \approx \varphi_N(n) + \arctan\left[\frac{B}{A_N}\sin(\varphi_Z(n) - \varphi_N(n))\right]$$

$$\approx \varphi_N(n) + \frac{B}{A_N}\sin(\varphi_Z(n) - \varphi_N(n)) \quad (22)$$

It is known that $\varphi_N(n)$ is fixed while $\varphi_Z(n)$ is a random value in the range [0, 2π]. Thus, the variance of $\eta(n)$ is expressed, according to the uncertainty propagation law, as:

$$\mathrm{Var}\{\eta(n)\} \approx \mathrm{Var}\left\{\varphi_N(n) + \frac{B}{A_N}\sin\left(\varphi_Z(n) - \varphi_N(n)\right)\right\}$$

$$\approx \mathrm{Var}\left\{\frac{B}{A_N}\sin\varphi_Z(n)\right\} \quad (23)$$

In light of the equation $\mathrm{Im}(V_Z(n)) = B\sin\varphi_Z(n)$, the following expression can be obtained:

$$\mathrm{Var}\{B\sin\varphi_Z(n)\} = \mathrm{Var}\{\mathrm{Im}(V_Z(n))\} = \frac{K\sigma^2}{2}NNPG \quad (24)$$

By considering the definition of the Equivalent Noise BandWidth (*ENBW*) of the EWF:

$$ENBW = \frac{NNPG}{\left[\dfrac{1}{K}\sum_{n=1}^{K}w_{eq}(n)\right]^2} = \frac{NNPG}{\left[\dfrac{1}{K}[H(0)]^L\right]^2} \quad (25)$$

The variance of $\eta(n)$ can be expressed under the assumption that $\Delta f \ll f_1$, $\omega_{1\text{-Neg}}(n) \approx 0$, as:

$$\mathrm{Var}\{\eta(n)\} \approx \left(\frac{2}{A_1}\right)^2 \frac{K\sigma^2 \cdot NNPG}{2[H(0)]^{2L}} \approx \frac{ENBW}{K \cdot SNR} \quad (26)$$

A. Influence of White Noise on Frequency Estimation

Based on (7) and (8), the variance of the estimated frequency can be represented by the variance of Δf as:

$$\mathrm{Var}\{f_1\} = \mathrm{Var}\{\Delta f\} = \left(\frac{Df_r}{M \cdot 2\pi}\right)^2 \cdot \mathrm{Var}\{\eta(n_2) - \eta(n_1)\}$$

$$= \left(\frac{Df_r}{M \cdot 2\pi}\right)^2 \cdot \Big[\mathrm{Var}\{\eta(n_2)\} + \mathrm{Var}\{\eta(n_1)\}$$

$$-2\mathrm{Cov}\{\eta(n_2),\eta(n_1)\}\Big] \quad (27)$$

where Cov{ } represents the covariance. Moreover, the values of $\mathrm{Var}\{\eta(n_1)\}$ and $\mathrm{Var}\{\eta(n_2)\}$ can be obtained according to the statistical characteristics of the AWGN approximately as:

$$\mathrm{Var}\{\eta(n_2)\} \approx \mathrm{Var}\{\eta(n_1)\}$$

$$\approx \mathrm{Var}\{\eta(n)\} \approx \frac{ENBW}{K \cdot SNR} \quad (28)$$

Due to that K is linearly proportional to both D and L, thus, according to (28), it results that $\mathrm{Var}\{\eta(n_1)\}$ and $\mathrm{Var}\{\eta(n_2)\}$ are inversely proportional to both D and L.

Then, the variance of the frequency is determined by the result of $\mathrm{Cov}\{\eta(n_2), \eta(n_1)\}$. Its result depends, according to the definition of covariance, on the overlap between n_1 and n_2, which can be described by two cases, $M \geq K$ and $M < K$.

Firstly, if $M \geq K$, there is no overlap between the raw samples of n_1 and n_2, thereby $\mathrm{Cov}\{\eta(n_2), \eta(n_1)\} = 0$ due to the characteristics of AWGN, and the variance of the frequency can be expressed as:

$$\mathrm{Var}\{f_1\} = \left(\frac{Df_r}{M \cdot 2\pi}\right)^2 \cdot \frac{2ENBW}{K \cdot SNR}$$

$$= \frac{(Df_r)^2}{2\pi^2 M^2 \cdot SNR} \cdot \frac{ENBW}{K} \quad (29)$$

Secondly, if $M < K$, there will be $K-M$ samples overlapping in the raw data between the two measuring points $n1$ and $n2$. For $L=1$, it is simple to obtain the relationship between $K-M$ and $\mathrm{Cov}\{\eta(n_2), \eta(n_1)\}$ due to the equality of the filter's weights. However, it becomes very complicated when $L \geq 2$, because the weights of the EWF are different one from each other. To solve this issue, an index named Overlap Correlation (*OC*) is introduced. This is to simplify the complex cases into a simple situation, as the relationship between the overlap samples and the value of $\mathrm{Cov}\{\eta(n_2), \eta(n_1)\}$ when $L=1$. The *OC* index is defined as [27]:

$$OC(\delta) = \frac{\displaystyle\sum_{n=1}^{\delta K}\left[w_{eq}(n)\,w_{eq}\left(n + (1-\delta)K\right)\right]}{\displaystyle\sum_{n=1}^{K}\left[w_{eq}(n)\right]^2} \quad (30)$$

where δ is the overlap coefficient, $\delta = (K-M)/K$. Therefore, the value of *OC* is constrained in $0 \leq OC \leq 1$.

Consequently, the $\mathrm{Cov}\{\eta(n_2), \eta(n_1)\}$ when $M < K$ can be approximately as:

$$\mathrm{Cov}\{\eta(n_2),\eta(n_1)\} \approx \frac{ENBW}{K \cdot SNR}OC(\delta) \quad (31)$$

Thus, the variance of the estimated frequency when $M < K$ can be expressed as:

$$\mathrm{Var}\{f_1\} = \frac{(Df_r)^2}{2\pi^2 M^2 \cdot SNR} \cdot \frac{ENBW}{K}\left(1 - OC(\delta)\right) \quad (32)$$

And (29) can be seen as the result of (32) when *OC* is 0 (which corresponds to the case $M \geq K$). Therefore, (32) can be considered as the frequency variance of FSF regardless of the overlap.

The *ENBW* and *OC* results of the EWF with different L, D and M are listed in Table II.

As can be seen from the Table, for a fixed D, the increment of the number of iterations L results in an increase in the *ENBW* and the *OC*. And for a fixed L and D, *OC* decreases when M increases. However, D has a very weak impact on the *ENBW* of EWF.

B. Comparison of Frequency Estimation to CRLB

For a frequency estimator, it is necessary to compare its variance with its CRLB which expresses a lower bound on the variance of unbiased estimators of a deterministic parameter. To fulfill the requirement of unbiased estimation when using FSF, the measurement interval M is set to K. Moreover, for a sufficiently large D, $K \approx LD$. Thus, the variance of the frequency can be simplified by starting from (29) as:

TABLE II THE *ENBW* AND *OC* OF EQUIVALENT WEIGHTING FILTER

| Number of Iterations	ENBW		OC			
	D=50	D=100	D=50, M=15	D=50, M=25	D=50, M=35	D=50, M=45
L=1	1.0000	1.0000	0.7000	0.5000	0.3000	0.1000
L=2	1.3203	1.3267	0.8852	0.7187	0.5221	0.3311
L=3	1.6283	1.6391	0.9215	0.7963	0.6381	0.4723
L=4	1.8890	1.9032	0.9392	0.8398	0.7092	0.5648
L=5	2.1181	2.1350	0.9504	0.8680	0.7571	0.6302
L=6	2.3246	2.3440	0.9581	0.8877	0.7914	0.6786
L=7	2.5142	2.5358	0.9637	0.9023	0.8173	0.7159
L=8	2.6905	2.7141	0.9680	0.9136	0.8375	0.7455
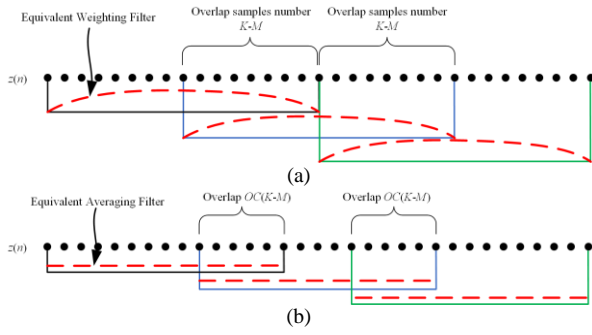
Fig. 1. The effect of *OC* on the overlap of two filters, (a) the number of overlapping samples is *K-M* when filtered by EWF, (b) by applying *OC*, the overlap in (a) can be equivalent to *OC(K-M)* samples overlapped under an equivalent averaging filter.

$$\text{Var}\{f_1\} = \frac{f_r^2}{2\pi^2} \cdot \frac{ENBW}{L^3 D} \cdot \frac{1}{SNR} \qquad (33)$$

It is significant that $ENBW/L^3D$ can influence the variance of the frequency, but also that the *ENBW* is closely related to the number of iterations *L*, which means that *L* is the key parameter for the frequency variance computation based on FSF.

According to [28] and concerning sinusoidal signals, the CRLB of the variance of an unbiased frequency estimation is given as:

$$CRLB = \frac{12\left(Df_r\right)^2}{\left(2\pi\right)^2 N\left(N^2 - 1\right)} \cdot \frac{1}{SNR} \qquad (34)$$

where *N* is the number of samples used, and it can be roughly assumed that $N=2LD$ when $M=K$. Hence, by replacing the expression of *N*, the CRLB of Var{f_1} can be obtained as:

$$CRLB \approx \frac{3}{4} \frac{f_r^2}{2\pi^2 L^3 D} \cdot \frac{1}{SNR} = \frac{3}{4} \cdot \frac{1}{ENBW} \cdot \text{Var}\{f_1\} \qquad (35)$$

As it emerges from (35), for unbiased frequency estimation of FSF, the ratio between the variance and its CRLB is equal to 4*ENBW*/3. Thus, we know that as *L* increases, the variance of the frequency estimation will move away from its CRLB because the *ENBW* increases as *L* increases.

IV. SIMULATIONS

To verify the effectiveness of the derived variance expression, some simulations with the Matlab software are carried out. A pure sinusoidal voltage signal corrupted by AWGN is employed. Different settings of FSF are used to estimate the frequency of the contaminated signal by applying (8). In the simulation, the variance of the power system frequency has been computed as:

$$\text{Var}_S\{f_1\} = \frac{1}{T}\sum_{i=1}^{T}\left(f_{1\text{-est}}(i) - \text{E}\{f_{1\text{-est}}\}\right)^2 \qquad (36)$$

where $f_{1\text{-est}}$ represents the estimated frequency by FSF; *T* is the number of estimates used to calculate the variance. Without loss of generality, *T* is set to 3000, which means each simulation variance is based on 3000 independent runs. As for the theoretical variances, they are directly provided by (32).

A. Simulation vs. SNR

TABLE III THE *ENBW*, *OC*, *K* AND *N* UNDER DIFFERENT SETTINGS OF (*L*, *M*)

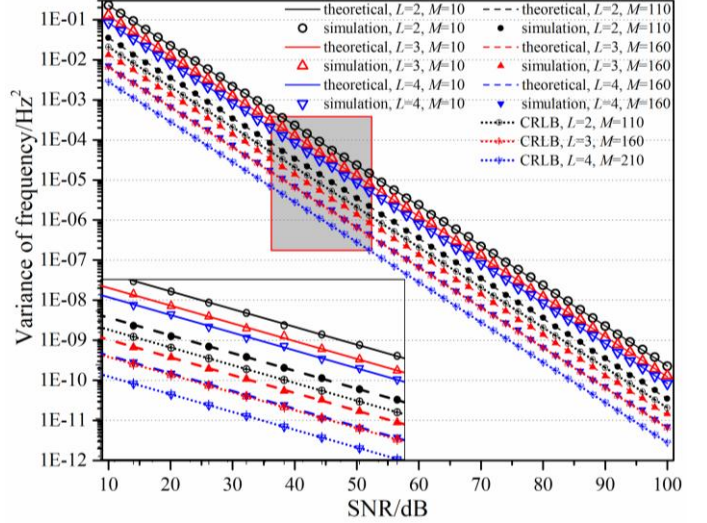| Settings of (*L*, *M*)	*K*	*ENBW*	*OC*	*N*
(2, 10)	99	1.3203	0.9460	109
(2, 110)	99	1.3203	0	209
(3, 10)	148	1.6283	0.9643	158
(3, 160)	148	1.6283	0	258
(4, 10)	197	1.8890	0.9725	207
(4, 210)	197	1.8890	0	307

Fig. 2. Variances of frequency estimates versus different SNRs, while *D*=50.

To verify the correctness of the proposed variance expression vs. different values of SNR, a sinusoidal voltage signal with frequency f_1=49.9 Hz, amplitude A_1=220 V and phase angle θ_1=10° is generated with zero mean white noise interference. For simplicity, the pure signal is marked as *X*. The SNR of white noise varies from 10 to 100 dB, with 2 dB steps. *D* and n_1 of FSF are fixed to 50 and 0, respectively, while the (*L*, *M*) couples are selected as (2, 10), (2, 110), (3, 10), (3, 160), (4, 10) and (4, 210). The length *K*, *ENBW* and *OC* of EWF under the simulation conditions, as well as the minimum number of samples required *N* are tabulated in Table III.

From the table, it is worth noting that, when *D* is fixed, an *L* variation generates different length *K* of EWF and different values of *ENBW*. The minimum number of samples *N*, determined by *L*, *D*, and *M*, can be obtained by *N=L(D-1)+1+M*. Moreover, for different *K*, same *M* can bring different *OC* due to the different overlap *K-M*. Thus, the selections of the (*L*, *M*) couples are divided into two cases, i.e., *OC*>0 (*M<K*) and *OC*=0 (*M≥K*). The simulation results of frequency variance in these two cases are displayed in Fig. 2. Whereas the corresponding CRLB is given in the figure when the settings of FSF fulfill the requirement of the unbiased estimation.

Fig. 2 compares the simulation and theoretical variances of frequency estimate versus different SNRs in the cases of *M<K* and *M>K*. According to Fig. 2, general conclusions can be summarized as follows. 1) The theoretical variances are consistent with the ones obtained from simulation, hence they confirm the correctness of the proposed frequency variance expression. 2) The variance of frequency estimation is inversely proportional to the SNR, which means the higher the

SNR, the smaller the variance. 3) The frequency variances are inversely proportional to the number of iterations L under fixed M and D. One thing should be underlined is that the number of the used samples N is different when L changes.

B. Simulation vs. Number of Iterations

According to (32), we know that the number of iterations L can affect the variance of the estimated frequency by changing the *ENBW*, K, and *OC*. To examine the effect of L on Var$\{f_1\}$ instead, the pure sinusoidal signal X corrupted by AWGN of SNR=65 dB has been adopted. The parameters of FSF are $D=50$, $n1=0$, L ranges from 1 to 8, M is selected to be 25 and $K=L(D-1)+1$, which corresponds to the cases of $OC>0$ and $OC=0$, respectively. The number of samples N is determined by $K+M$. The simulation results are listed in Table IV.

The comparison between the simulation and theoretical variance confirms again the validity of the proposed variance expression. More can be found in Table IV is that, regardless of the overlap, the increase of L leads to an increment of *ENBW* and K but a reduction of frequency variance. According to (32), we know that *ENBW* is proportional to the Var$\{f_1\}$ while K is inversely proportional to the Var$\{f_1\}$. Because that the increase rate of K is higher than that of *ENBW* when L increases, the Var$\{f_1\}$ decreases. This phenomenon can also be found from the simulation results of $\{1\}$, $\{1,1\}$, $\{1,1,1\}$, $\{1,1,1,1\}$, and $\{1,1,1,1,1\}$ in figure 11 of [18]. However, the increase of K implies more time delay and heavier computational burden. Thus, it is a trade-off to select a suitable L for frequency estimation according to the requirement of the measurement.

C. Simulation Performed Varying the Measurement Interval

It is interesting that, under the same measurement conditions, frequency variance of FSF depends on the variation of measurement interval M since the frequency is estimated by the angle difference of two samples with measurement interval M. Thus, to evaluate the FSF-based frequency variance with different M is significant. For this purpose, signal X is generated and then measured under the condition of M varying from 1 to 301, with steps of 4. The SNR of the superimposed white noise is 65 dB and 85 dB, while the number of iterations L is set to 2, 3 and 4, respectively. The other parameters of FSF are $n1=0$, $D=50$. The results of all the combination obtained are shown in Fig. 3.

In the picture, the theoretical and simulation variance results of different M values show good agreement. It is worth noting that in Fig. 3, the theoretical variances of frequency are obtained in two cases, $1\le M<K$ and $M\ge K$, the specific value of K corresponding to different L can be found in Table III. Furthermore, it can be seen from Fig. 3 that, for a specific L, the Var$\{f_1\}$ decreases as M increases due to the inverse relationship between Var$\{f_1\}$ and M. For a specific SNR, the differences between the variances of different L to each other are larger when M is relatively small. When M increases, the differences between the variances are gradually reduced. That is because, the dominator of Var$\{f_1\}$ changes from $(1-OC)ENBW/K$ to $ENBW/M^2$ when M increases. In addition, higher SNR can reduce the frequency variance.

TABLE IV INFLUENCE OF L ON FREQUENCY ESTIMATION WITH AWGN

| L	Simulation, $M=25$	Theoretical, $M=25$	*ENBW*	K
1	1.59E-06	1.60E-06	1.0000	50
2	6.77E-07	6.01E-07	1.3203	99
3	3.59E-07	3.59E-07	1.6283	148
4	2.49E-07	2.46E-07	1.8890	197
5	1.87E-07	1.82E-07	2.1181	246
6	1.42E-07	1.42E-07	2.3246	295
7	1.15E-07	1.14E-07	2.5142	344
8	9.89E-08	9.48E-08	2.6905	393
	Simulation, $M=K$	Theoretical, $M=K$	*ENBW*	K
1	8.05E-07	8.01E-07	1.0000	50
2	1.42E-07	1.36E-07	1.3203	99
3	4.96E-08	5.03E-08	1.6283	148
4	2.45E-08	2.47E-08	1.8890	197
5	1.47E-08	1.42E-08	2.1181	246
6	9.00E-09	9.07E-09	2.3246	295
7	6.13E-09	6.18E-09	2.5142	344
8	4.40E-09	4.44E-09	2.6905	393
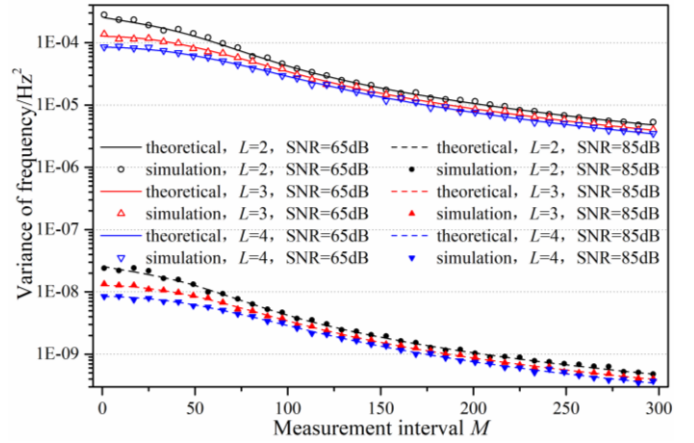
Fig. 3. Variances of frequency estimates versus different measurement interval M and SNRs, while D is fixed to 50.
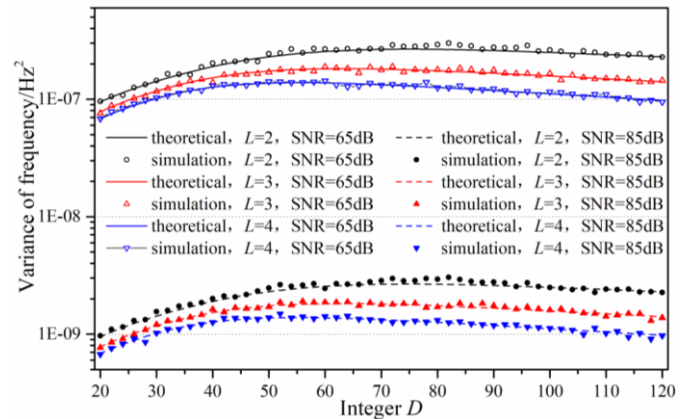

Fig. 4. Variances of frequency estimates versus different number of samples in one period D and SNRs, while M is fixed to 75.

D. Simulations Performed Varying the Samples Number

The number of samples in one period D produces a significant effect on the frequency estimation under noisy condition because both K and *ENBW* are D dependent. Thus, it

is of importance to test the influence of D on the FSF-based frequency variance under the pollution of white noise. To this end, X has been adopted to perform simulations when D varies linearly from 20 to 120 with steps of 2. The SNR of AWGN is set to 65 dB and 85 dB. The L values employed are 2, 3 and 4. The other parameters are set as $n1=0$ and $M=75$. Fig. 4 depicts the variances of frequency versus variation of D, obtained from the simulation.

Also from Fig. 4 results, the theoretical and simulation variances still agree with each other, and lower SNR produces higher frequency variance. From the figure, it can be found that, in the case where SNR, M, and L are unchanged, the frequency variance first increases faster when D increases, and then slowly decreases. The explanation of the phenomenon can be that, with fixed SNR, M and L, the main determinant of frequency variance is roughly $D(1-OC)$ according to (32). Notice that, the variation of $D(1-OC)$ only depends on D when $M \geq K$ since OC is 0 in this case. While $M<K$, the effect of D on OC should be considered, thereby the value of $D(1-OC)$ is a coaction result of variations of D and the OC.

E. Simulation vs. Frequency Deviation and Harmonic

The power system signal always suffers from frequency deviation and harmonics. To evaluate the performance of the proposed frequency variance expression under the condition of frequency deviation and harmonics, the pure signal shown in Table V is generated with AWGN of SNR=63dB. The simulation condition is, $D=50$, $n_1=0$, $M=25$, $L=3$ and 4. The fundamental frequency f_1 varies from 48 Hz to 52 Hz, with a step of 0.1 Hz. The results of the simulation and theoretical frequency variances are compared in Fig. 3. As a contrast, the simulation results of a pure sinusoidal wave of $A_1=220$ V, $\theta_1=10\,°$are also provided.

In Fig. 5, it can see that, when the frequency deviation between f_1 and f_r is not so large, approximately within 0.5 Hz, the theoretical and simulation variances match well which means (26) can be guaranteed when $|\Delta f| \leq 0.5$Hz. As for the harmonic, there is no evidence from Fig. 5 that it has an impact on FSF-based frequency variance.

F. Simulations for Variance vs. CRLB Comparison

The CRLB expresses a lower bound on the variance of unbiased estimators of a deterministic parameter which plays an important role in uncertainty analysis. In section III, part B, the comparison between the FSF-based variance and its CRLB is analyzed theoretically. To verify the theoretical conclusion, the following simulations are carried out. The signal $v1$ has been employed likewise. The simulation conditions are, $n1=0$, $D=50$, $L=2$, 3 and 4. As for the measurement interval M, it has been chosen accordingly to meet the requirement of unbiased estimation, i.e., for $L=2$, $M=99$, for $L=3$, $M=148$, for $L=4$, $M=197$. The simulation variance and the corresponding CRLB with different measurement conditions are listed in Table IV, along with the simulation ratios and the theoretical ones. It is worth noting that the simulation ratios are the values of $\mathrm{Var_S}\{f_1\}/\mathrm{CRLB}$ whereas the latter ones are calculated by using $4ENBW/3$.

TABLE V PARAMETERS OF THE HARMONICS

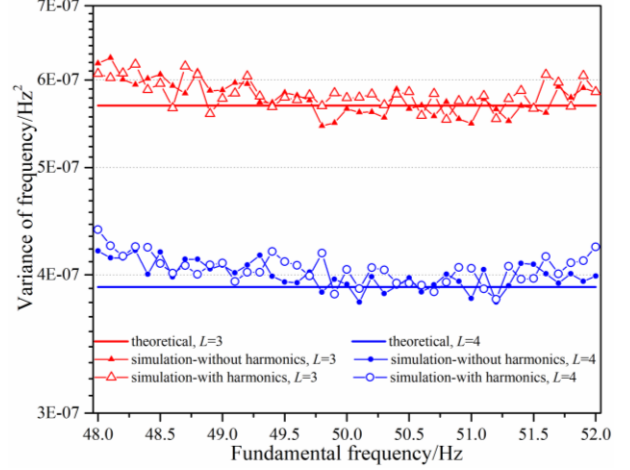| h	1	2	3	4	5
A_h(V)	220	3	17	2	10
θ_h(°)	10	20	30	40	50

Fig. 5. Frequency variance under frequency deviation and harmonics.

TABLE VI COMPARISON BETWEEN THE VARIANCE AND ITS CRLB

(L, SNR)	Simulation Variance	CRLB	Simulation Ratio	Theoretical Ratio
(2, 30)	4.55E-04	2.45E-04	1.8590	1.7603
(2, 60)	4.35E-07	2.45E-07	1.7776	1.7603
(2, 90)	4.61E-10	2.45E-10	1.8831	1.7603
(3, 30)	1.61E-04	7.33E-05	2.2008	2.1710
(3, 60)	1.57E-07	7.33E-08	2.1432	2.1710
(3, 90)	1.65E-10	7.33E-11	2.2522	2.1710
(4, 30)	8.13E-05	3.11E-05	2.6159	2.5187
(4, 60)	7.91E-08	3.11E-08	2.5474	2.5187
(4, 90)	7.76E-11	3.11E-11	2.4988	2.5187

In light of the results in Table IV, it can be stated that the deduced ratio is fully comparable with the actual one. This reflects the correctness of the proposed expression either. Another aspect that needs to be mentioned is that, as the number of iterations L increases, the ratio between the variance and its CRLB increases, which means that the increment of L leads to a higher discrepancy between the variance and its CRLB, viz. the effectiveness of the frequency estimator is reduced as the increment of L.

V. CONCLUSION

The FSF-based frequency variance is related to the interval between two adopted measuring points, since the selection of the measurement interval determines the overlap of the raw samples. By introducing the Equivalent Noise Bandwidth and Overlap Correlation of the EWF, the influence of white noise on FSF-based power system frequency estimation is studied and presented in this paper. The expression of frequency variance is derived and presented theoretically with respect to SNR. Moreover, the ratio between the frequency variance and its CRLB is given. The correctness of the proposed expression is validated by the designed simulations. According to the proposed frequency variance expression, with fixed sampling frequency, the accuracy level of FSF-based frequency

estimation of the noisy signal will increase by increasing the number of iterations and the measurement interval. However, the increment of measurement interval will increase the time delay directly while the computational burden and the time delay will both increase as the increment of the number of iterations. Thus, a suitable selection of the measurement interval and the number of iterations should be determined according to the requirement of the measurement.

REFERENCES

[1] X. Hui, M. Wang, R. Yang, and Z. Yan, "Power System Frequency Estimation Method in the Presence of Harmonics," *IEEE Transactions on Instrumentation & Measurement,* vol. 65, no. 1, pp. 56-69, 2016.

[2] S. Schuster, S. Scheiblhofer, and A. Stelzer, "The Influence of Windowing on Bias and Variance of DFT-Based Frequency and Phase Estimation," *IEEE Transactions on Instrumentation & Measurement,* vol. 58, no. 6, pp. 1975-1990, 2009.

[3] B. Jafarpisheh, S. M. Madani, F. Parvaresh, and S. M. Shahrtash, "Power System Frequency Estimation Using Adaptive Accelerated MUSIC," *IEEE Transactions on Instrumentation & Measurement,* vol. 67, no. 11, pp. 2592-2602, 2018.

[4] S. K. Jain and S. N. Singh, "Low-Order Dominant Harmonic Estimation Using Adaptive Wavelet Neural Network," *IEEE Transactions on Industrial Electronics,* vol. 61, no. 1, pp. 428-435, 2013.

[5] C. J. Ramos, A. P. Martins, and A. S. Carvalho, "Frequency and phase-angle estimation using ordinary least squares," *IEEE Transactions on Industrial Electronics,* vol. 62, no. 9, pp. 5677-5688, 2015.

[6] J. A. D. L. O. Serna, "Polynomial Implementation of the Taylor–Fourier Transform for Harmonic Analysis," *IEEE Transactions on Instrumentation & Measurement,* vol. 63, no. 12, pp. 2846-2854, 2014.

[7] M. Karimi-Ghartemani, A. R. Bakhshai, and M. Mojiri, "Estimation of Power System Frequency Using Adaptive Notch Filter," *IEEE Transactions on Instrumentation & Measurement,* vol. 56, no. 6, pp. 2470-2477, 2005.

[8] Z. Feng, Z. Huang, C. Zhao, X. Wei, and D. Chen, "Time-Domain Quasi-Synchronous Sampling Algorithm for Harmonic Analysis Based on Newton's Interpolation," *IEEE Transactions on Instrumentation & Measurement,* vol. 60, no. 8, pp. 2804-2812, 2011.

[9] D. Belega and D. Petri, "Accuracy of the Synchrophasor Estimator Returned by the Interpolated DFT Algorithm Under Off-Nominal Frequency and Harmonic Conditions," in *2018 IEEE 9th International Workshop on Applied Measurements for Power Systems (AMPS)*, 2018, pp. 1-6: IEEE.

[10] Q. Hao, R. Zhao, and C. Tong, "Interharmonics Analysis Based on Interpolating Windowed FFT Algorithm," *IEEE Transactions on Power Delivery,* vol. 22, no. 2, pp. 1064-1069, 2007.

[11] J. Zhang, W. He, T. Lu, Z. Teng, and C. Zhou, "Frequency Shifting And Filtering Algorithm for Power System Harmonic Estimation," in *IEEE International Workshop on Applied Measurements for Power Systems*, 2017.

[12] Z. Shuai, J. Zhang, L. Tang, Z. Teng, and H. Wen, "Frequency shifting and filtering algorithm for power system harmonic estimation," *IEEE Transactions on Industrial Informatics,* 2018.

[13] A. Mingotti, L. Peretto, and R. Tinarelli, "Uncertainty Analysis of an Equivalent Synchronization Method for Phasor Measurements," *IEEE Transactions on Instrumentation & Measurement,* vol. PP, no. 99, pp. 1-9.

[14] A. Mingotti, L. Peretto, R. Tinarelli, and K. Yigit, "Simplified Approach to Evaluate the Combined Uncertainty in Measurement Instruments for Power Systems," *IEEE Transactions on Instrumentation & Measurement,* vol. 66, no. 9, pp. 2258-2265, 2017.

[15] L. Zhan, Y. Liu, J. Culliss, J. Zhao, and Y. Liu, "Dynamic Single-Phase Synchronized Phase and Frequency Estimation at the Distribution Level," *IEEE Transactions on Smart Grid,* vol. 6, no. 4, pp. 2013-2022, 2015.

[16] Z. Jin and H. Zhang, "Noise characteristics and fast filtering of synchronized frequency measurement in low voltage grid," in *Smart Energy Grid Engineering*, 2016.

[17] H. Wen, C. Li, and W. Yao, "Power system frequency estimation of sine-wave corrupted with noise by windowed three-point interpolated DFT," *IEEE Transactions on Smart Grid,* vol. 9, no. 5, pp. 5163-5172, 2018.

[18] A. J. Roscoe, S. M. Blair, B. Dickerson, and G. Rietveld, "Dealing With Front-End White Noise on Differentiated Measurements Such as Frequency and ROCOF in Power Systems," *IEEE Transactions on Instrumentation and Measurement,* no. 99, pp. 1-13, 2018.

[19] R. Ghiga, K. Martin, Q. Wu, and A. Nielsen, "Phasor Measurement Unit Test under Interference Conditions," *IEEE Transactions on Power Delivery,* vol. 33, no. 2, pp. 630-639, 2018.

[20] V. Friedman, "A zero crossing algorithm for the estimation of the frequency of a single sinusoid in white noise," *IEEE Transactions on Signal Processing,* vol. 42, no. 6, pp. 1565-1569, 2002.

[21] A. Routray, A. K. Pradhan, and K. P. Rao, "A novel Kalman filter for frequency estimation of distorted signals in power system," *IEEE Transactions on Instrumentation & Measurement,* vol. 51, no. 3, pp. 469-479, 2002.

[22] C. Offelli and D. Petri, "The influence of windowing on the accuracy of multifrequency signal parameter estimation," *IEEE Transactions on Instrumentation and Measurement,* vol. 41, no. 2, pp. 256-261, 1992.

[23] D. Belega and D. Petri, "Influence of the Noise on DFT-based Sine-wave Frequency and Amplitude Estimators," *Measurement,* 2019.

[24] H. Wen, S. Guo, Z. Teng, F. Li, and Y. Yang, "Frequency estimation of distorted and noisy signals in power systems by FFT-based approach," *IEEE Transactions on Power Systems,* vol. 29, no. 2, pp. 765-774, 2014.

[25] D. Bellan, "Detection and estimation of weak sine waves with random offset and additive noise," in *International Conference on Instrumentation*, 2013.

[26] K. H. Jin and P. N. Markham, "Power System Frequency Estimation by Reduction of Noise Using Three Digital Filters," *IEEE Transactions on Instrumentation & Measurement,* vol. 63, no. 2, pp. 402-409, 2014.

[27] F. J. Harris, "On the use of windows for harmonic analysis with the discrete Fourier transform," *Proceedings of the IEEE,* vol. 66, no. 1, pp. 51-83, 1978.

[28] S. M. Kay, *Fundamentals of statistical signal processing*. Prentice Hall PTR, 1993.

Junhao Zhang (S'17) was born in Henan, China, in 1986. He received the B.Sc. degree from Hunan University in 2009. He is currently working toward the Ph.D. degree in the College of Electrical and Information Engineering, Hunan University, Hunan, China. His research interests include electrical measurement and digital signal processing.

Lu Tang received his B.Sc. and M.Sc. degree from Huazhong University of Science and Technology, and his Ph.D degree from Academy 0f Mathematics and Systems Science, Chinese Academy of Sciences (CAS). Since 2007, he has been a Lectuer in Hunan University, his main interest and research field are power system analysis, signal processing and complex systems.

A. Mingotti (S'17) was born in Cento (FE), Italy in 1992. He received the B.S. and the M.S. degrees in electrical engineering from the University of Bologna (Italy), in 2014 and 2016, respectively. He is currently pursuing the PhD degree in biomedical, electrical, and system engineering at the University of Bologna under the supervision of Prof. Lorenzo Peretto. His research interests include management and condition maintenance of distribution networks, development, modelling, and metrological characterization of instrument transformers.

L. Peretto (M'98, SM'03) is a Professor of Electrical and Electronic Measurements at the University of Bologna, Italy. He is Senior Member of IEEE and member of the IEEE Instrumentation and Measurement Society. He is Chairman of the annual IEEE Applied Measurements for Power System Conference, member of the IEC TC38 "Instrument Transformers" and Chairman of the TC38/WG45 "Standard Mathematical Models for Instrument Transformers" and of the TC38/WG53 "Uncertainty evaluation in the calibration of Instrument Transformers".

His fields of research are the design and calibration of voltage and current instrument transformers (LPIT) for medium and high voltage power networks; the design and realization of calibration systems of voltage and current instrument transformers; measurements of electrical quantities in power networks.

He is author and co-author of more than 200 papers and of 24 patents and co-author of three books. He is consultant of industries operating in the field of instrumentation and sensors for electrical measurements.

He Wen (M'12) was born in Hunan, China, in 1982. He received the B.Sc., M.Sc, and Ph.D. degrees in electrical engineering from Hunan University, Hunan, China, in 2004, 2007, and 2009, respectively. He is currently a full professor with the College of Electrical and Information Engineering, Hunan University, China. His present research interests include electrical contact reliability, wireless communications, power system harmonic measurement and analysis, power quality, and digital signal processing. Also, he is the deputy director of Hunan Province Key Laboratory of Intelligent Electrical Measurement and Application Technology.

He is an Associate Editor of the IEEE TRANSACTIONS ON INSTRUMENTATION AND MEASUREMENT, and a Member of Editorial Board of FLUCTUATION AND NOISE LETTERS.